

Coordinative Unsaturation versus Oxophilicity: *ansa* Dimethylsilyl Oxo-Bridged Uranium Metallocenes. Synthesis, Structures, and Unexpected Catalytic Activity with Alkynes and Silanes

Jiayi Wang,^{†,‡} Ylia Gurevich,[†] Mark Botoshansky,[†] and Moris S. Eisen^{*,†}

Schulich Faculty of Chemistry and Institute of Catalysis Science and Technology, Technion–Israel Institute of Technology, Haifa, 32000, Israel, and Institute of Polymer Science and Engineering, Hebei University of Technology, Tianjin, 300130, People's Republic of China

Received May 9, 2008

The tetrachloride salt of uranium reacts with 1 equiv of the lithium ligand $\text{Li}_2[(\text{C}_5\text{Me}_4)_2\text{SiMe}_2]$ in DME to form the complex $[\eta^5-(\text{C}_5\text{Me}_4)_2\text{SiMe}_2]\text{UCl}_2 \cdot 2\text{LiCl} \cdot 2\text{DME}$ (**1**), which undergoes a rapid hydrolysis either in DME with equimolar amounts of water to give the coordinatively unsaturated bridged monooxide and monochloride uranium lithium salt complex $\{[\eta^5-(\text{C}_5\text{Me}_4)_2\text{SiMe}_2]\text{UCl}\}_2(\mu\text{-O})(\mu\text{-Cl}) \cdot \text{Li}(\text{DME})_3 \cdot \text{DME}$ (**2**) or in toluene to yield the dimeric bridged monochloride monooxide lithium salt complex $\{[\eta^5-(\text{C}_5\text{Me}_4)_2\text{SiMe}_2]\text{UCl}\}_2(\mu\text{-O})(\mu\text{-Cl}) \cdot \text{Li} \cdot 1/2\text{DME}\}_2$ (**3**). Alkylation of either complex **2** or **3** with BuLi in DME gives the monobridged dibutyl complex $\{[\eta^5-(\text{C}_5\text{Me}_4)_2\text{SiMe}_2]\text{UBu}\}_2(\mu\text{-O})$ (**4**). Complex **2** was characterized by solid state X-ray analysis. Complex **4** was found to be an active catalyst for the disproportionation metathesis of $\text{TMSC}\equiv\text{CH}$ and the cross-metathesis of $\text{TMSC}\equiv\text{CH}$ or $\text{TMSC}\equiv\text{CTMS}$ with various terminal alkynes. To shed some light on the possible mechanistic scenario, different alkynes, $\text{TMSC}\equiv\text{CH}$, $\text{TMSC}\equiv\text{CTMS}$, or $\text{TMSC}\equiv\text{CPr}^t$, were reacted in the presence of complex **4** with PhSiH_3 , producing a myriad of products in addition to the unexpected TMSH and SiH_4 (*caution*), indicating the cleavage of the trimethylsilyl group from the alkyne and the formation of a uranium-silyl intermediate. Complex **4** was also found to be an active catalyst for the phenyl cleavage metathesis of PhSiH_3 to form Ph_2SiH_2 and Ph_3SiH . In C_6D_6 solutions, the C–D activation of the aromatic ring takes place, forming $\text{C}_6\text{D}_5\text{SiH}_3$. Plausible mechanisms for all the catalytic processes are presented.

Introduction

During the last two decades, the chemistry of electrophilic d^0/f^n actinide compounds has been the source of intense investigations and reached a high level of sophistication.¹ The broad interest of these compounds originates from their unique structure–reactivity relationships and their remarkable performances in homogeneous catalysis.² It has been well established that the stability and reactivity of almost all the organometallic complexes of the d- and especially of the f-elements are exceedingly sensitive to the ancillary ligands that are bonded

to the metal center.^{1–4} The usefulness of the pentamethylcyclopentadienyl ligation in affording simple actinide complexes with advantageous solubility, thermal stability, and resistance to ligand redistribution has been recognized in the last two decades.^{1,3} However, in order to open the actinide coordination sphere while preserving the frontier orbital of these advantageous ligands, the actinide coordination chemistry of the bridged ligation $\text{Me}_2\text{Si}(\text{C}_5\text{Me}_4\text{H})_2$ has been explored.⁴ Organometallic complexes of the f-elements are known to be especially sensitive to moisture, and the decomposition products are generally assumed to be oxo-bridged derivatives. These compounds are normally difficult to prepare owing to the difficult control of

* Corresponding author. E-mail: chmoris@tx.technion.ac.il.

[†] Technion–Israel Institute of Technology.

[‡] Hebei University of Technology.

(1) (a) Barnea, E.; Eisen, M. S. *Coord. Chem. Rev.* **2006**, *250*, 855. (b) Barnea, E.; Andrea, T.; Berthet, J.-C.; Ephritikhine, M.; Eisen, M. S. In *Recent Advances in Actinide Science*; Alvarez, R.; Bryan, N. D.; May, I., Eds.; RSC Publishing: Manchester, UK, 2006; pp 163–167. (c) Barnea, E.; Moradove, D.; Berthet, J.-C.; Ephritikhine, M.; Eisen, M. S. In *Recent Advances in Actinide Science*; Alvarez, R.; Bryan, N. D.; May, I., Eds.; RSC Publishing: Manchester, UK, 2006; pp 234–236. (d) Burns, C. J.; Eisen, M. S. In *The Chemistry of the Actinide and Transactinide Elements*, 3rd ed.; Morss, L. R.; Edelstein, N.; Fuger, J., Eds.; Springer: Berlin, 2006; pp 2799–2910. (e) Burns, C. J.; Eisen, M. S. In *The Chemistry of the Actinide and Transactinide Elements*, 3rd ed.; Morss, L. R.; Edelstein, N.; Fuger, J., Eds.; Springer: Berlin, 2006; pp 2911–3012. (f) Andrea, T.; Eisen, M. S. *Chem. Soc. Rev.* **2008**, *37*, 550. (g) Sharma, M.; Eisen, M. S. *Struct. Bonding (Berlin)* **2008**, *127*, 1–85. (h) Lam, O. P.; Feng, P. L.; Heinemann, F. W.; O'Connor, J. M.; Meyer, K. *J. Am. Chem. Soc.* **2008**, *130*, 2806, and references therein. (i) Evans, W. J.; Kozimor, S. A.; Ziller, J. W. *Science* **2005**, *309*, 1835. (j) Hayton, T. W.; Boncella, J. M.; Scott, B. L.; Palmer, P. D.; Batista, E. R.; Hay, P. *J. Science* **2005**, *310*, 1941. (k) Summerscales, O. T.; Cloke, F. G. N.; Hitchcock, P. B.; Green, J. C.; Hazari, N. *Science* **2006**, *311*, 829.

(2) (a) Bruno, J. W.; Smith, G. M.; Marks, T. J. *J. Am. Chem. Soc.* **1986**, *108*, 40. (b) Smith, G. M.; Carpenter, J. D.; Marks, T. J. *J. Am. Chem. Soc.* **1986**, *108*, 6805. (c) Lin, Z.; Marks, T. J. *J. Am. Chem. Soc.* **1990**, *112*, 5515. (d) Gillespie, R. D.; Burwell, R. L., Jr.; Marks, T. J. *Langmuir* **1990**, *6*, 1465. (e) Chen, Y. X.; Metz, M. V.; Li, L.; Stern, C. L.; Marks, T. J. *J. Am. Chem. Soc.* **1998**, *120*, 6287. (f) Jia, L.; Yang, X.; Stern, C. L.; Marks, T. J. *Organometallics* **1997**, *16*, 842. (g) Wang, J. X.; Dash, A. K.; Berthet, J. C.; Ephritikhine, M.; Eisen, M. S. *J. Organomet. Chem.* **2000**, *610*, 49. (h) Andrea, T.; Barnea, E.; Eisen, M. S. *J. Am. Chem. Soc.* **2008**, *130*, 2454.

(3) Mark, T. J.; Streitwiser, A., Jr. In *The Chemistry of the Actinide Element*, 2nd ed.; Katz, J. J., Seaborg, G. T., Morss, L. R., Eds.; Chapman and Hall: London, 1986; Chapter 22.

(4) (a) Fendrick, C. M.; Mintz, E. A.; Schertz, L. D.; Mark, T. J.; Day, V. W. *Organometallics* **1984**, *3*, 819. (b) Jeske, G.; Schock, L. E.; Swepston, P. N.; Schumann, H.; Marks, T. J. *J. Am. Chem. Soc.* **1985**, *107*, 8103. (c) Fendrick, C. M.; Schertz, L. D.; Day, V. W.; Marks, T. J. *Organometallics* **1988**, *7*, 1828. (d) Schnabel, R. C.; Scott, B. L.; Smith, W. H.; Burns, C. J. *J. Organomet. Chem.* **1999**, *591*, 14. (e) Dash, A. K.; Gourevich, I.; Wang, J. Q.; Wang, J.; Kapon, M.; Eisen, M. S. *Organometallics* **2001**, *20*, 5084.

the partial hydrolysis for a given precursor.⁵ Rarely those complexes are just formed from their recrystallization in the presence of useful trace amounts of water.⁵ While bridging oxide uranium(IV) complexes are still relatively rare,⁶ it would be very interesting to know their structural and, if possible, their catalytic properties for these bridged f-complexes due to their expected highly open coordination sphere. It has been pointed out that molecular compounds with a M–O–M skeleton (M = metal) may serve as a model for oxide-supported heterogeneous organometallic catalysts or metal-oxide-containing catalysts.⁷ The presence of metal–oxide bonds usually reduces the sensitivity of these complexes toward oxygen and moisture. For neutral organoactinides, catalyzed reactions were first limited to C–H activation and hydrogenation. Hence, for example, the hydrogenation performed with alkoxylated organoactinide complexes has been found to have much lower reactivity as compared to the corresponding hydride complexes.⁸

During the last decade we have considered new catalytic reactions using organoactinides. Hydroamination,⁹ oligomerization,¹⁰ selective dimerizations,¹¹ hydrosilylation of alkynes,¹² coupling of isonitriles with alkynes,¹³ and the unexpected polymerization of lactones¹⁴ comprise part of these processes. Interestingly, the oxygen-bridged dibutyl uranium complex has

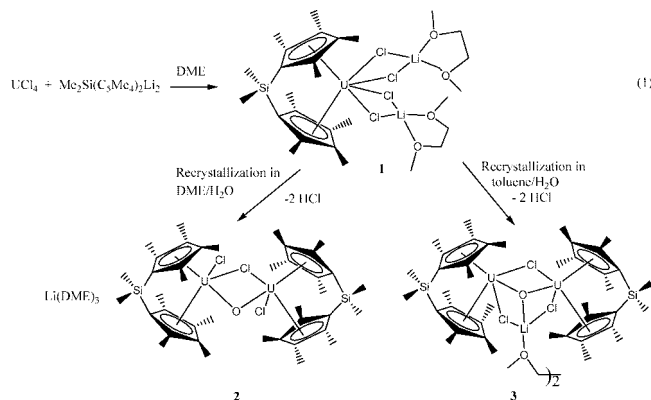
been found to be an active catalyst for the disproportionation metathesis of $\text{TMSC}\equiv\text{CH}$ and the cross-metathesis of $\text{TMSC}\equiv\text{CH}$ or $\text{TMSC}\equiv\text{CTMS}$ with various terminal alkynes.¹⁵

In this contribution we present the synthesis and X-ray diffraction studies for an oxide-bridged uranium complex, **2**, and the catalytic activity of the corresponding oxide-bridged dibutyl uranium complex, **4**, obtained from either complex **2** or **3** upon its reaction with butyllithium. Unique metathesis reactions of this active complex with internal and terminal silylalkynes with PhSiH_3 produce a myriad of products in addition to TMSH , SiH_4 , Ph_2SiH_2 , and Ph_3SiH . The reaction of complex **4** with PhSiH_3 is also presented in different solvents, and a C–D activation is observed in C_6D_6 . Plausible mechanisms for the formation of the different compounds are proposed.

Results and Discussion

Synthesis of Oxo-Bridged Uranium Complexes **2** and **3**.

The reaction of UCl_4 with the lithium salt $\text{Me}_2\text{Si}(\text{C}_5\text{Me}_4)_2\text{Li}_2$ in DME yields the organouranium chloride complex **1** (eq 1), which was isolated as an air- and moisture-sensitive orange powder. The complex was prepared following the protocol published for the synthesis of a similar dark red uranium complex containing diethyl ether, thf, or TMEDA instead of DME.^{4d} Interestingly, the spectroscopic analysis of both (DME and diethyl ether) complexes was found to be almost identical.



The oxo-bridged organouranium complex **2** and the oxo-bridged organouranium complex **3** were obtained from planned reactions of complex **1** in either DME or toluene, in the presence of stoichiometric amounts of water, respectively. When stoichiometric amounts are used, no free ancillary ligand is observed in solution; however, if larger amounts of water are used, the free ligand is detached from the metal center and mixtures of compounds are obtained. The ^1H NMR spectrum of complex **2** is peculiar, consisting of two fully discrete sets of isotropically shifted, narrow resonances for C_5Me_4 and Me_2Si (a total of 10 different methyl signals). Furthermore, the ^{13}C NMR of complex **2** shows, unexpectedly, only one signal for each methyl for the four C_5Me_4 moieties and one signal for both methyl groups in the two Me_2Si groups. This result is an outcome of the paramagnetic shift effect of the uranium, having two f-electrons that influence the ligand hydrogens strongly as compared to their corresponding carbons.¹⁶ For complex **3** the ^1H and ^{13}C NMR are extremely broad presumably due to the

(5) (a) Lukens, W. W.; Beshouri, S. M.; Bloesch, L. L.; Andersen, R. A. *J. Am. Chem. Soc.* **1996**, *118*, 901. (b) Zalkin, A.; Beshouri, S. M. *Acta Crystallogr., Sect. C: Cryst. Struct. Commun.* **1988**, *C44*, 1826. (c) Brianese, N.; Casellato, U.; Ossola, F.; Porchia, M.; Rossetto, G.; Zanella, P.; Graziani, R. *J. Organomet. Chem.* **1989**, *365*, 223. (d) Berthet, J. C.; Ephritikhine, M.; Lance, M.; Nierlich, M.; Vigner, J. *J. Organomet. Chem.* **1993**, *460*, 47. (e) Evans, W. J.; Seibel, C. A.; Forrestal, K. J.; Ziller, J. W. *J. Coord. Chem.* **1999**, *48*, 403. (f) Spirlet, M. R.; Rebizant, J.; Apostolidis, C.; Dornberger, E.; Kanellakopulos, B.; Powietzka, B. *Polyhedron* **1996**, *15*, 1503.

(6) (a) Rebizant, J.; Spirlet, M. R.; Apostolidis, C.; Kanellakopulos, B. *Acta Crystallogr., Sect. C: Cryst. Struct. Commun.* **1992**, *C48*, 452. (b) Berthet, J. C.; Le Marechal, J. F.; Nierlich, M.; Lance, M.; Vigner, J.; Ephritikhine, M. *J. Organomet. Chem.* **1991**, *408*, 335. (c) Cramer, R. E.; Bruck, M. A.; Gilje, J. W. *Organometallics* **1988**, *7*, 1465. (d) Herrmann, W. A.; Anwander, R.; Kleine, M.; Oefele, K.; Riede, J.; Scherer, W. *Chem. Ber.* **1992**, *125*, 2391. (e) Berg, D. J.; Burns, C. J.; Andersen, R. A.; Zalkin, A. *Organometallics* **1989**, *8*, 1865. (f) Schumann, H.; Palamidis, E.; Loebel, J. *J. Organomet. Chem.* **1990**, *384*, C49. (g) Beeckman, W.; Goffart, J.; Rebizant, J.; Spirlet, M. R. *J. Organomet. Chem.* **1986**, *307*, 23–7.

(7) (a) Evans, W. J.; Grate, J. W.; Bloom, I.; Hunter, W. E.; Atwood, J. L. *J. Am. Chem. Soc.* **1985**, *107*, 405, and references therein. (b) Eisen, M. S.; Marks, T. J. *J. Am. Chem. Soc.* **1992**, *114*, 10358. (c) Eisen, M. S.; Marks, T. J. *Organometallics* **1992**, *11*, 3939. (d) Eisen, M. S.; Marks, T. J. *J. Mol. Catal.* **1994**, *86*, 23.

(8) Lin, Z.; Marks, T. J. *J. Am. Chem. Soc.* **1987**, *109*, 7979.

(9) (a) Haskel, A.; Straub, T.; Eisen, M. S. *Organometallics* **1996**, *15*, 3773. (b) Straub, T.; Frank, W.; Reiss, G. J.; Eisen, M. S. *J. Chem. Soc., Dalton Trans.* **1996**, 2541. (c) Eisen, M. S.; Straub, T.; Haskel, A. *J. Alloys Compd.* **1988**, *271–273*, 116. (d) Straub, T.; Haskel, A.; Neyroud, T. G.; Kapon, M.; Botoshansky, M.; Eisen, M. S. *Organometallics* **2001**, *20*, 5017. (e) Stubbert, B. D.; Marks, T. J. *J. Am. Chem. Soc.* **2007**, *129*, 4253. (f) Stubbert, B. D.; Stern, C. L.; Marks, T. J. *Organometallics* **2003**, *22*, 4836.

(10) (a) Straub, T.; Haskel, A.; Eisen, M. S. *J. Am. Chem. Soc.* **1995**, *117*, 6364. (b) Haskel, A.; Straub, T.; Dash, A. K.; Eisen, M. S. *J. Am. Chem. Soc.* **1999**, *121*, 3014. (c) Wang, J.; Dash, A. K.; Kapon, M.; Berthet, J. C.; Ephritikhine, M.; Eisen, M. S. *Chem.–Eur. J.* **2002**, *8*, 5384. (d) Wang, J. Q.; Dash, A. K.; Berthet, J. C.; Ephritikhine, M.; Eisen, M. S. *Organometallics* **1999**, *18*, 2407. (e) Dash, A. K.; Wang, J. Q.; Berthet, J. C.; Ephritikhine, M.; Eisen, M. S. *J. Organomet. Chem.* **2000**, *604*, 83.

(11) Haskel, A.; Wang, J. Q.; Straub, T.; Gueta-Neyroud, T.; Eisen, M. S. *J. Am. Chem. Soc.* **1999**, *121*, 3025.

(12) (a) Dash, A. K.; Wang, J. Q.; Eisen, M. S. *Organometallics* **1999**, *18*, 4724. (b) Eisen, M. S. In *The Chemistry of Organosilicon Compounds*; Appeloig, Y.; Rappoport, Z., Eds.; John Wiley: Chichester, Vol. 2, Part 3, 1998; p 2038. (c) Eisen, M. S. *Rev. Inorg. Chem.* **1997**, *17*, 25. (d) Wang, J.; Gurevich, Y.; Botoshansky, M.; Eisen, M. S. *J. Am. Chem. Soc.* **2006**, *128*, 9350.

(13) (a) Barnea, E.; Andrea, T.; Kapon, M.; Berthet, J. C.; Ephritikhine, M.; Eisen, M. S. *J. Am. Chem. Soc.* **2004**, *126*, 10860. (b) Barnea, E.; Andrea, T.; Berthet, J.-C.; Ephritikhine, M.; Eisen, M. S. *Organometallics* (in press).

(14) Barnea, E.; Moradove, D.; Berthet, J. C.; Ephritikhine, M.; Eisen, M. S. *Organometallics* **2006**, *25*, 320.

(15) Wang, J.; Gurevich, Y.; Botoshansky, M.; Eisen, M. S. *J. Am. Chem. Soc.* **2006**, *128*, 9350.

(16) Morril, T. C. In *Lanthanide Shift Reagents in Stereochemical Analysis*; John Wiley & Sons: New York, 1987; pp 1–209.

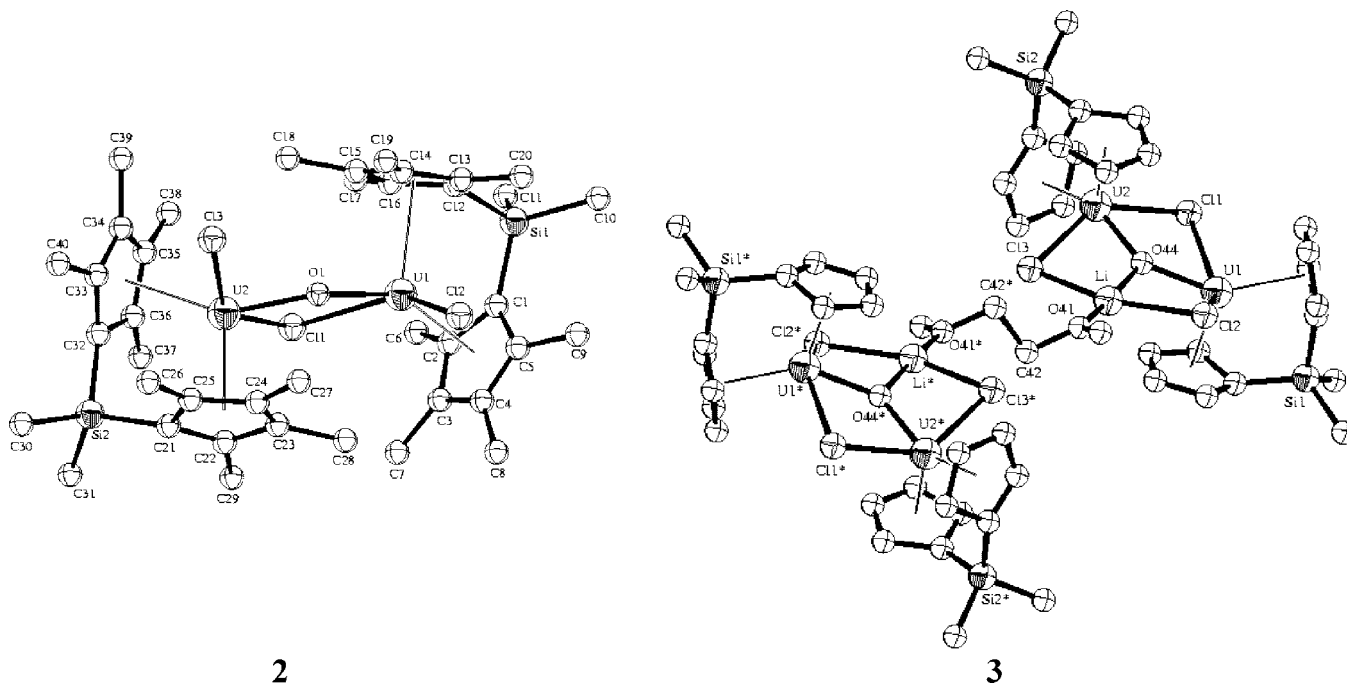


Figure 1. ORTEP plot of the molecular structure of complex $\{[\eta^5\text{-}(\text{C}_5\text{Me}_4)_2\text{SiMe}_2\text{UCl}]_2(\mu\text{-O})(\mu\text{-Cl})\cdot\text{Li}(\text{DME})_3\cdot\text{DME}$ (**2**). The ORTEP plot of the octahedral $\text{Li}(\text{DME})_3$ moiety corresponding to complex **2** was omitted from the figure for clarity, and $\{[\eta^5\text{-}(\text{C}_5\text{Me}_4)_2\text{SiMe}_2\text{UCl}]_2(\mu\text{-O})(\mu\text{-Cl})\text{Li}\cdot\text{O}(\text{CH}_3)_2\text{CH}_2\}_2$ (**3**) was drawn at the 50% probability level (methyls at Cp rings are omitted for clarity). In addition, all hydrogen atoms and DME crystal inclusion molecules were also omitted for clarity.

Table 1. Crystal Data Collection for Complexes **2** and **3**

	2	3
empirical formula	$\text{C}_{56}\text{H}_{100}\text{Cl}_3\text{LiO}_9\text{Si}_2\text{U}_2$	$\text{C}_{42}\text{H}_{65}\text{Cl}_3\text{LiO}_2\text{Si}_2\text{U}_2$
space group	$C2/c$	$P 21/c$
temperature (K)	220(2)	230(1)
unit cell dimens a (Å)	34.896(4)	15.052(3)
b (Å)	9.6010(11)	10.636(2)
c (Å)	39.433(4)	28.982(6)
α (deg)	90	90
β (deg)	103.359(7)	97.33(3)
γ (deg)	90	90
V (Å ³)	12854(3)	4601.9(16)
Z	8	4
density(calcd) (mg/m ³)	1.615	1.801
absorp coeff (mm ⁻¹)	5.244	7.288
$F(000)$	6192	2396
cryst size (mm)	0.22 × 0.17 × 0.04	0.15 × 0.08 × 0.08
θ range for data collection (deg)	2.12 to 25.00	1.42 to 25.00
index ranges	$0 \leq h \leq 41, -11 \leq k \leq 11, -46 \leq l \leq 45$	$-17 \leq h \leq 17, -12 \leq k \leq 12, -34 \leq l \leq 23$
no. of refls collected	28 640	22 823
no. of indep refls	11 222 ($R_{\text{int}} = 0.0590$)	7888 ($R_{\text{int}} = 0.1020$)
refinement method	full-matrix least-squares on F^2	full-matrix least-squares on F^2
no. of data/restraints/params	11 222/0/634	7888/0/472
goodness of fit on F^2	0.819	0.944
final R indices $R1 [I > 2\sigma(I)]$	$R1 = 0.0477, wR2 = 0.0787$	$R1 = 0.0650, wR2 = 0.1167$
R indices (all data)	$R1 = 0.1356, wR2 = 0.0836$	$R1 = 0.1677, wR2 = 0.1513$
largest diff peak and hole ($e \text{ \AA}^{-3}$)	1.574 and -1.090	1.399 and -1.938

combination of the strong paramagnetic shifts obtained by the four different uranium (f^2) metal centers.^{15,16}

Molecular Structure Characterization for $\{[\eta^5\text{-}(\text{C}_5\text{Me}_4)_2\text{SiMe}_2\text{UCl}]_2(\mu\text{-O})(\mu\text{-Cl})\cdot\text{Li}(\text{DME})_3\cdot\text{DME}$ (2**) and $\{[\eta^5\text{-}(\text{C}_5\text{Me}_4)_2\text{SiMe}_2\text{UCl}]_2(\mu\text{-O})(\mu\text{-Cl})\text{Li}\cdot\text{O}(\text{CH}_3)_2\text{CH}_2\}_2$ (**3**).** The molecular structure of complex **2** has been confirmed by X-ray single-crystal diffraction studies. The ORTEP plot of the complex is shown in Figure 1, and crystallographic data with structure refinement details and selected bond lengths and angles are listed in Tables 1 and 2, respectively.

In complex **2**, the two uranium atoms are bridged by an oxygen atom and a chlorine atom, forming an almost planar

$\text{U}_1\text{O}_1\text{U}_2\text{Cl}_1$ four-membered ring, which is slightly puckered through the vector $\text{O}-\text{Cl}$ with a maximum deviation of 0.0126 Å from the ideal plane. In addition, each metal is also bound to one additional chlorine atom. The terminal $\text{U}-\text{Cl}$ distances of U_1-Cl_2 (2.692(3) Å) and U_2-Cl_3 (2.680(3) Å) are comparable to typical $\text{U}-\text{Cl}$ distance (e.g., 2.687(4) Å in $\text{LiU}_2\text{Cl}_5(\text{CH}_2\text{-}(\text{C}_5\text{H}_4)_2)_2\cdot 2\text{THF}$,¹⁷ 2.681(1) Å in $[(\text{C}_5\text{Me}_5)_2\text{UCl}]_2\text{O}^{6d}$). The bond lengths for the bridged uranium-chloride U_1-Cl_1 (2.838(3) Å) and U_2-Cl_1 (2.866(3) Å) are much larger compared to the

(17) Secaur, C. A.; Day, V. W.; Ernst, R. D.; Kennelly, W. J.; Marks, T. J. *J. Am. Chem. Soc.* **1976**, *98*, 3713.

Table 2. Selected Bond Lengths (Å) and Angles (deg) for Complexes $[\{\eta^5\text{-}(\text{C}_5\text{Me}_4)_2\text{SiMe}_2\text{UCl}\}_2(\mu\text{-Cl})(\mu\text{-O})\cdot\text{Li}(\text{DME})_3\cdot\text{DME}$ (**2**) and $[\{\{\eta^5\text{-}(\text{C}_5\text{Me}_4)_2\text{SiMe}_2\text{UCl}\}_2(\mu\text{-O})(\mu\text{-Cl})\text{Li}\cdot\text{O}(\text{CH}_3)_2\text{CH}_2\}_2]$ (**3**)

2		3	
Bond Lengths			
U ₁ –Cl ₁	2.838(3)	U ₁ –Cl ₁	2.830(4)
U ₁ –Cl ₂	2.692(3)	U ₁ –Cl ₂	2.732(4)
U ₁ –O ₁	2.127(5)	U ₁ –O ₄₄	2.145(9)
U ₂ –Cl ₁	2.900(3)	U ₂ –Cl ₁	2.830(4)
U ₂ –Cl ₃	2.680(3)	U ₂ –Cl ₃	2.709(5)
U ₂ –O ₁	2.027(5)	U ₂ –O ₄₄	2.157(10)
Bond Angles			
2		3	
Cl ₁ –U ₁ –Cl ₂	142.57(8)	Cl ₃ –U ₂ –Cl ₁	136.87(13)
O ₁ –U ₁ –Cl ₁	65.53(17)	O ₄₄ –U ₁ –Cl ₂	76.4(3)
O ₁ –U ₁ –Cl ₂	84.38(17)	O ₄₄ –U ₂ –Cl ₃	75.2(2)
O ₁ –U ₂ –Cl ₁	67.96(17)	U ₂ –Cl ₁ –U ₁	88.24(12)
O ₁ –U ₂ –Cl ₃	83.72(17)		
Cl ₁ –U ₂ –Cl ₃	143.06(7)		
U ₂ –Cl ₁ –U ₁	85.90(8)		
U ₂ –O ₁ –U ₁	138.6(3)		

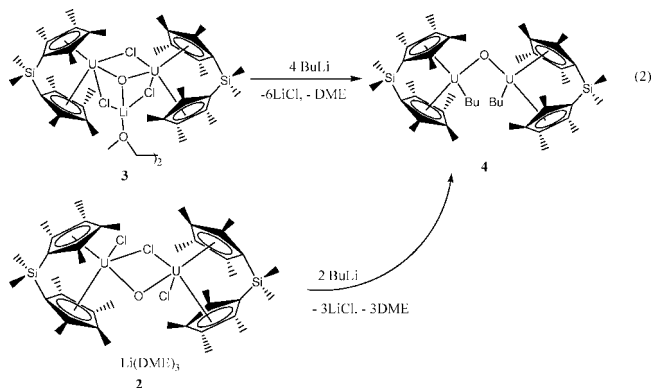
terminal U–Cl bond lengths, although comparable to bridging chlorides in other uranium complexes (2.885(3) and 2.853(3) Å in $\text{Me}_2\text{Si}(\text{C}_5\text{Me}_4)_2\text{U}(\mu\text{-Cl}_4)\{\text{Li}(\text{TMEDA})\}_2$,^{4d} 2.821(1) and 2.841(1) Å in $\text{LiU}_2\text{Cl}_5(\text{CH}_2(\text{C}_5\text{H}_4)_2)_2\cdot 2\text{THF}$. The metal–oxygen U₁–O₁ (2.127(6) Å) and U₂–O₁ (2.027(7) Å) bond lengths are similar and are in the range found for other U–O bridging complexes (2.131(4), 2.125(4) Å in $[(\text{C}_5\text{Me}_5)_2\text{U}]_2\text{O}$,^{6c} 2.053(6) Å in $\{\text{U}(\text{C}_5\text{H}_4\text{SiMe}_3)_2(\mu\text{-O})\}_3$,^{6c}) and almost identical to the dimeric complex of uranium(IV) $[(1,3\text{-}(\text{CH}_3)_3\text{Si})_2\text{C}_3\text{H}_3)_2\text{U}\text{-O}]_2$ (2.096(6) and 2.129(5) Å).^{6a} The disposition of the bridging oxide and chloride atoms is almost symmetrical toward the two uranium metal centers. Complex **2** contains two bridging $\text{Me}_2\text{Si}(\text{C}_5\text{Me}_4)_2$ units having four different tetramethylcyclopentadienyl rings (Cp'). To be able to compare each of the Cp' rings, due to their large asymmetry toward the metals, we have averaged the distance of each of the carbons at each cyclopentadienyl moiety to the corresponding metal. Thus Cp₁' represents the ring C(1)–C(5) (span range from 2.719 to 2.919 Å), Cp₂' represents the ring C(12)–C(16) (span range from 2.707 to 2.828 Å), Cp₃' represents the ring C(21)–C(25) (span range from 2.741 to 2.799 Å), and Cp₄' represents the ring C(32)–C(36) (span range from 2.764 to 2.900 Å). The four different metal–Cp' average distances obtained are U₁–Cp₁' (2.819 Å), U₂–Cp₂' (2.767 Å), U₁–Cp₃' (2.770 Å), and U₂–Cp₄' (2.832 Å). Noteworthy to point out is that at each uranium unit one of the Cp' rings of the bridged chelating ligand is closer to the metal than the other Cp'. This result affects the disposition of the terminal chlorine atoms, which are closer to the cyclopentadienyl rings Cp₁' and Cp₄', causing the asymmetric environment. The asymmetry is an outcome of the octahedral lithium moieties that are disposed close to these two Cp' motifs through the unit cell.

The molecular structure of complex **3** has been confirmed by X-ray single-crystal diffraction studies. The ORTEP plot of the complex is shown in Figures 1 and 2, and crystallographic data with structure refinement details and selected bond lengths and angles are listed in Tables 1 and 2, respectively. Two different types of chlorine atoms are found in each unit of the dimeric complex **3**, as found in the X-ray structure (Figure 2).¹⁵ A bridging chloride is between two uranium metals, and two additional bridge chlorides are between the uranium metals and the lithium center. In the former bridge, the U–Cl distances U(1)–Cl(1) (2.842(6) Å) and U(2)–Cl(1) (2.824(6) Å) are longer than U(1)–Cl(2) (2.732(4) Å) and U(2)–Cl(3) (2.692(7)

Å) but in the normal range found for other bridging chloride atoms between uranium metals or in complex **2**.^{4,17}

The molecular structures of both complexes **2** and **3** reveal typical bent metallocene complexes in regard to the ancillary cyclopentadienyl ligation. The ring centroid–U–centroid angles in complex **2** (114.68°, 115.45°) and in complex **3** (116.9°, 114.8°) are similar, as well as for other bridged uranium metallocene complexes such as in $\text{U}(\text{SiMe}_2(\text{C}_5\text{Me}_4)_2)\text{-Cl}_4\text{Li}_2\cdot 4\text{Et}_2\text{O}$ (114.1°)^{4b} or in $\{\text{Me}_2\text{Si}(\text{C}_5\text{Me}_4)(\text{C}_5\text{H}_4)\text{U}(\mu\text{-NPh})\}_2$ (115.5°).^{4d} The average Cp'–U distances following the number criteria as explained above for complex **3** are Cp₁'(C1–C5)–U(1) = 2.487 Å, Cp₂'(C13–17)–U(1) = 2.529 Å, Cp₃'(C21–C25)–U(2) = 2.454 Å, Cp₄'(C32–36)–U(1) = 2.492 Å and are in the normal range for other *ansa*-type uranium complexes but much shorter than in complex **2**.

Synthesis of the Oxo-Bridged Organouranium Butyl Derivative 4. Alkylation of complex **2** or **3** with 2 or 4 equiv of *n*-butyllithium, respectively, at –78 °C in THF proceeds smoothly to give the alkyl uranium complex **4** as a dark brown air- and moisture-sensitive solid (eq 2). The complex is slightly soluble in methylcyclohexane, benzene, and toluene and dissolves readily in THF or other ethereal solvents. The ¹H NMR spectrum of this paramagnetic f² uranium complex in THF-*d*₈ is complex, exhibiting large paramagnetic contact signals for the ancillary ligation $\text{Me}_2\text{Si}(\text{C}_5\text{Me}_4)_2$ and coordinated THF solvent molecules. The signals of the two butyl groups are broad and nonequivalent due to the plausible nonsymmetric coordination formed by the coordinated THF. In benzene, the signals are much better behaved, and it is possible to correlate the signals to the complex. Our attempts to get suitable single crystals of complex **4** for X-ray analysis were until now unsuccessful.



Although the elemental analysis of the complex is excellent, it was extremely important to prove the presence of the two butyl groups. To corroborate the existence of these alkyl moieties, we have reacted complex **4** with excess amounts of PhSiH_3 (eq 3), producing *only* 2 equiv of the corresponding PhSiH_2Bu . This result corroborates the presence of the two butyl groups as described in complex **4**. Any attempts to crystallize the hydride complex or to get an informative NMR have been unsuccessful. Only cryoscopic measurements of the “in situ” solution of the hydride complex in frozen benzene solutions have shown a $M_w = 1150 \pm 10\%$ (M_w calc for a monomer = 1091). It is important to point out that the formation of various complexes of dimeric and/or possible oligomeric nature, as found for other organoactinide hydride complexes, existing in equilibrium and in small amounts, can be the reason for the difference between the correct molecular weight and the found

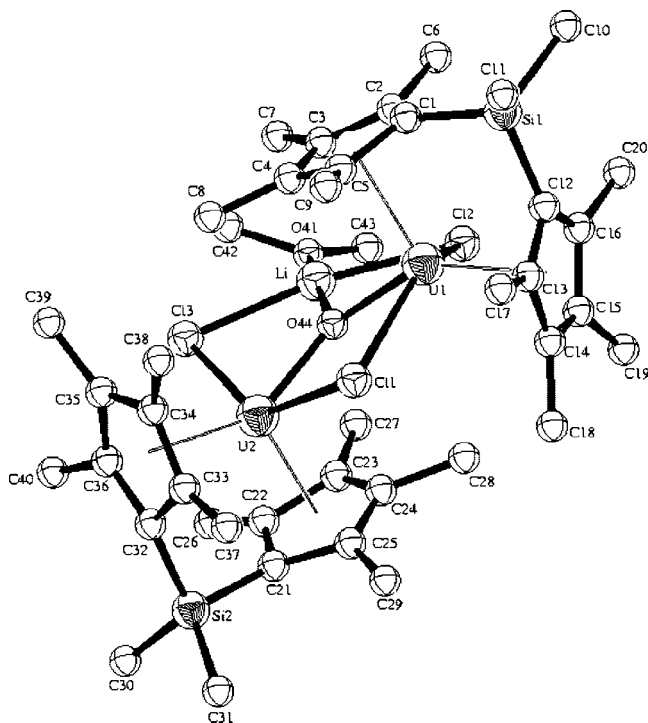
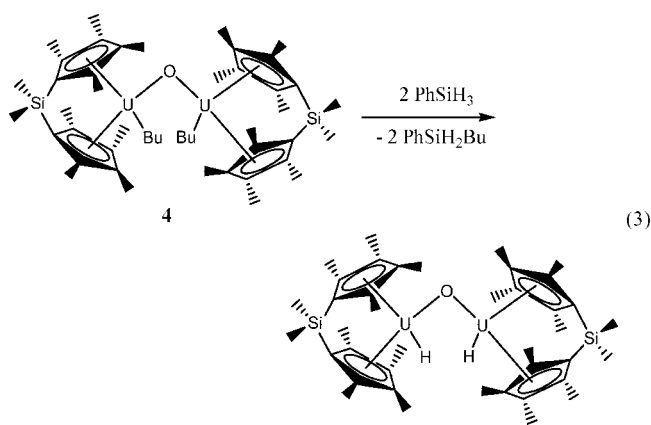


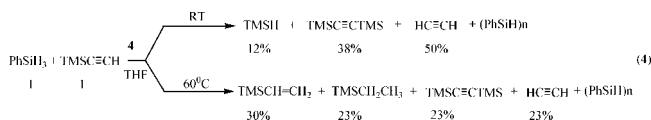
Figure 2. ORTEP plot of complex **3** showing the planar disposition of atoms Cl1, U1, U2, O41, and O44.



one.¹⁸ Moreover, the reaction of the in situ hydride complex (after evaporating PhSiH_2Bu under high vacuum and at room temperature) with D_2O produced almost stoichiometric amounts of HD, which were trapped and measured using a Toepler pump.

As we have already recently reported, complex $\text{Cp}^*_2\text{U}(\text{Me})_2$ is a good precatalyst for the hydrosilylation of alkynes and alkenes.^{4c} It was very interesting to compare the reactivity of complex **4**, having a bridging oxygen group, to the uranium metallocene (theoretically, a slow reactivity was expected), and specifically in its catalytic performance for the hydrosilylation of terminal alkynes. Hence, the reaction of $\text{TMSC}\equiv\text{CH}$ with PhSiH_3 in equimolar amounts or in slight excess of the latter, promoted by complex **4** in a THF solution, at room temperature produced, to our surprise, a mixture of compounds depending on time and temperature. At room temperature, TMSH, $\text{HC}\equiv\text{CH}$, and $\text{TMSC}\equiv\text{CTMS}$ were the major products with trace amounts

of the alkene $\text{TMSCH}=\text{CHTMS}$ (eq 4). In addition, follow-up of the reaction shows that at the first stages of the reaction small amounts of the dehydrogenative coupling of the silane product $\text{PhSiH}_2\text{H}_2\text{SiPh}$ were obtained,^{2r} and as the reaction continues, this dimer is consumed to form higher oligomers. After prolonged reaction periods, when all the $\text{TMSC}\equiv\text{CH}$ was consumed, the ratio $\text{TMSH}:\text{TMSC}\equiv\text{CTMS}:\text{HC}\equiv\text{CH}$ was nearly 1:3:4. Furthermore, 24% of the PhSiH_3 remained in solution and the reacted 76% was found to be *not incorporated* into the alkyne products but rather transformed to larger oligomers (dimers, trimers, or even Ph_2SiH_2 was not detected at long reaction periods).



When the reaction was carried out at 60 °C instead of at room temperature, the $\text{TMSC}\equiv\text{CH}$ was fully consumed, rapidly producing 30% of the hydrogenation alkene product $\text{TMSCH}=\text{CH}_2$, 23% of the fully hydrogenated alkane $\text{TMSCH}_2\text{CH}_3$, and 23% of each of the compounds $\text{TMSC}\equiv\text{CTMS}$ and $\text{HC}\equiv\text{CH}$. In addition, trace amounts of TMSH and silicon-incorporated alkane, alkene, and alkyne products $\text{TMSCH}_2\text{CH}_2\text{-SiH}_2\text{Ph}$, $\text{TMSCH}=\text{CHSiH}_2\text{Ph}$, and $\text{TMSC}\equiv\text{CSiH}_2\text{Ph}$,¹⁹ respectively, were observed in the GC-MS, and their detection was confirmed when compared to pure analytical materials.²⁰ At the culmination of the reaction when all the $\text{TMSC}\equiv\text{CH}$ was reacted, 25% of the PhSiH_3 still remains unreacted and about 74% of the silane yields oligomers as produced when the reaction was carried out at room temperature (eq 4).

A plausible mechanism explaining the formation of the alkyne part of the different products in the reaction of $\text{TMSC}\equiv\text{CH}$ in the presence of PhSiH_3 catalyzed by complex **4** is presented in Scheme 1.¹⁵ The mechanism presented consists of a sequence of elementary well-established steps, such as insertions, metathesis, and protonolysis-metal involving reactions.¹⁵ The first step of the catalytic cycle involves the rapid reaction of the starting complex **4** with the terminal acetylene to form the corresponding uranium acetylide complex **A** and 2 equiv of butane. A similar reactivity has been found in the oligomerization or hydrosilylation of terminal alkynes by different organoactinide complexes.^{9–12} Complex **A** reacts in a four-centered transition state with an additional $\text{TMSC}\equiv\text{CH}$, cleaving the Si–C bond and forming the internal alkyne $\text{TMSC}\equiv\text{CTMS}$ and the corresponding $\text{U}-\text{C}\equiv\text{CH}$ complex, as presented in complex **B**. The consecutive protonolysis reaction of complex **B** with another molecule of $\text{TMSC}\equiv\text{CH}$ regenerates complex **A** and forms the obtained acetylene $\text{HC}\equiv\text{CH}$. We have already disclosed this mechanism recently for the σ -bond metathesis of silylalkynes in the absence of silanes.¹⁵

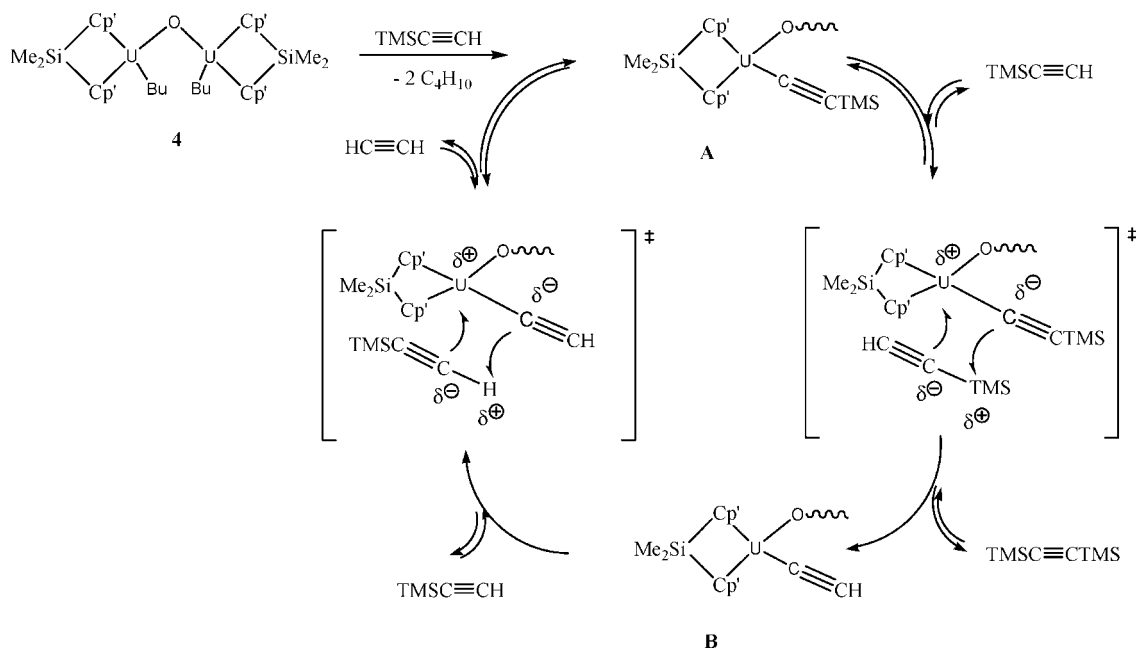
On the basis of this mechanism, equimolar amounts of the internal alkyne and acetylene should have been obtained (38% of each one). Consequently, it is reasonable that a second mechanism is operative, in parallel, responsible for the additional equimolar (12%) amounts of the TMSH and acetylene.

If either complex **A** or **B** reacts with PhSiH_3 , complex **C** will be formed, which upon additional reaction with PhSiH_3 , will form the corresponding hydride complex **D**^{9–11} and the formation of oligomeric products from the dehydrogenative coupling

(18) (a) Fagan, P. J.; Manriquez, J. M.; Maatta, E. A.; Seyam, A. M.; Marks, T. J. *J. Am. Chem. Soc.* **1981**, *103*, 6650. (b) Broach, R. W.; Schultz, A. J.; Williams, J. M.; Brown, G. M.; Manriquez, J. M.; Fagan, P. J.; Marks, T. J. *Science* **1979**, *203*, 172. (c) Manriquez, J. M.; Fagan, P. J.; Marks, T. J. *J. Am. Chem. Soc.* **1978**, *100*, 3939.

(19) The mechanistic pathways for the formation of $\text{TMSCH}_2\text{CH}_2\text{-SiH}_2\text{Ph}$, $\text{TMSCH}=\text{CHSiH}_2\text{Ph}$, and $\text{TMSC}\equiv\text{CSiH}_2\text{Ph}$ have been already disclosed for actinides. See ref 12.

(20) See Experimental Section.

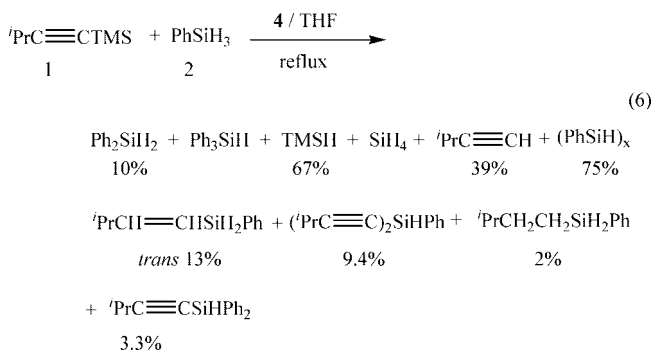
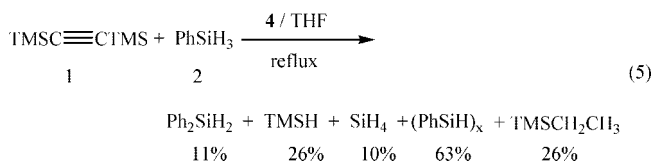
Scheme 1. Possible Equilibrium Mechanism for the Disproportionation of $\text{TMSC}\equiv\text{CH}$ Promoted by Complex **4**^a

of the silanes (Scheme 2). It is important to point out that complex **D** is also formed from the reaction of complex **4** and PhSiH_3 . From competitive studies at room temperature for this stage alone, we have found that complex **4** reacts faster (ca. $\times 3$) with the terminal alkyne than with the silane; hence both mechanisms will complement each other. Therefore, when complex **D** is formed from complex **B**, $\text{HC}\equiv\text{CH}$ is formed and the consecutive reaction of complex **D** with $\text{TMSC}\equiv\text{CH}$ produces equimolar amounts of TMSH and $\text{HC}\equiv\text{CH}$, regenerating complex **B**.

At higher temperature (eq 4), the phenylsilane is more active than the terminal alkyne (ca. $\times 10$), which produces more complex **D**, PhSiH_2Bu , and the polysilane. The hydride complex **D** prefers to undergo a σ -bond metathesis with a terminal alkyne, allowing the formation of the alkene complex **E** (almost no TMSH is formed), which reacts with PhSiH_3 , producing the alkene and complex **C**. Upon a consecutive reaction with an additional molecule of PhSiH_3 , complex **C** regenerates complex **D**. When the alkene inserts into the hydride complex **D** once again, the metathesis with an additional equivalent of PhSiH_3 will produce the fully hydrogenated alkane and regenerate again complex **D** (Scheme 3). In addition, no hydrogenation products of $\text{TMSC}\equiv\text{CTMS}$ were observed, indicating that the hydrogenation of the $\text{TMSC}\equiv\text{CH}$ is indeed much faster.

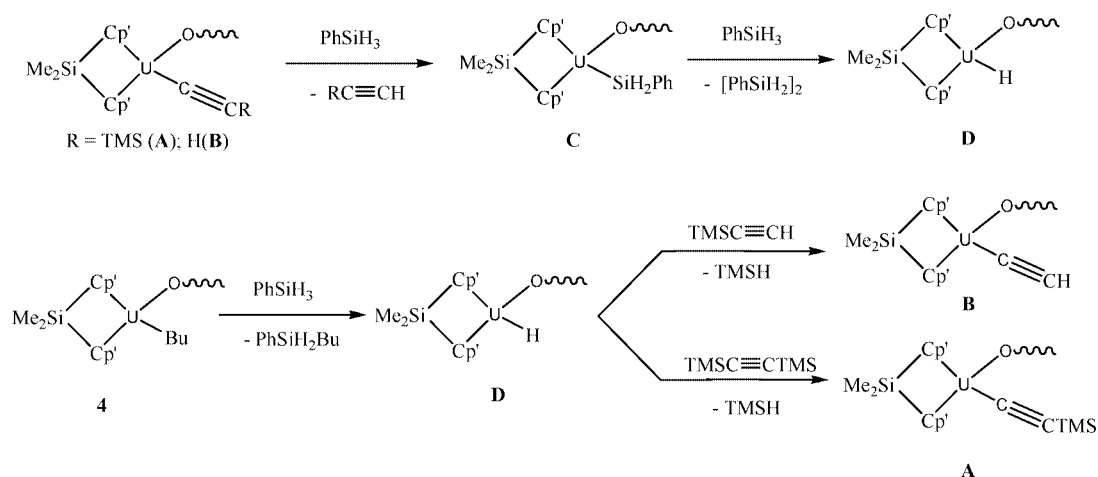
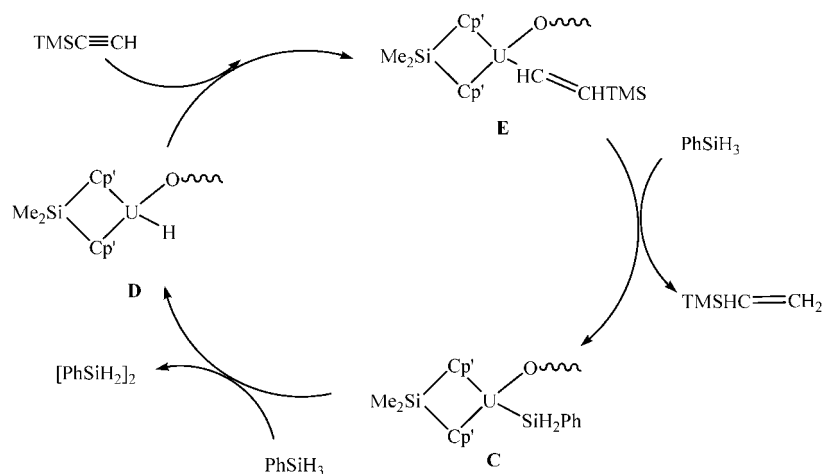
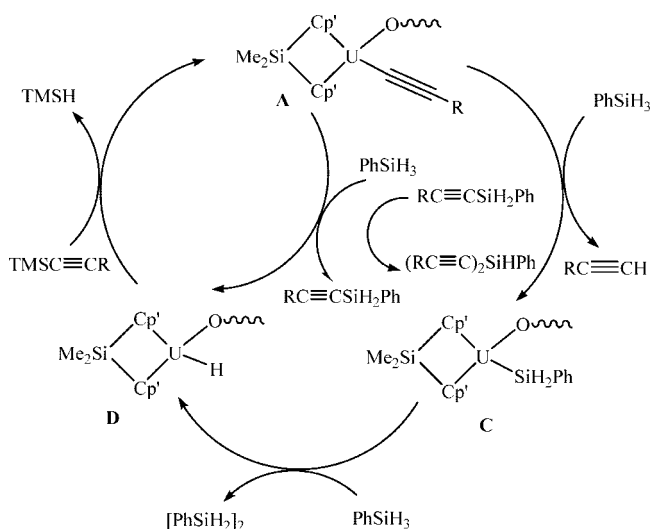
It was conceptually interesting, as well as challenging, to study the reactivity scope of complex **4** when the reaction is carried out between *internal alkynes* ($\text{TMSC}\equiv\text{CTMS}$ or $\text{TMSC}\equiv\text{CPr}^i$) as a source of TMS groups and PhSiH_3 as the hydride source for the production of a metal hydride.¹² Due to the complexity of the reaction, we quantified the products based on the starting material. The reaction of $\text{TMSC}\equiv\text{CTMS}$ with PhSiH_3 (1:2, respectively) promoted by complex **4**, in refluxing THF solution, for 47 h, produces 63% oligomers via the dehydrogenative coupling of silanes, 11% Ph_2SiH_2 , and 10% SiH_4 (*Caution, extremely flammable compound*). In addition, 26% of $\text{TMSC}\equiv\text{CTMS}$ yields equimolar amounts of TMSH (26%) and $\text{TMSCH}_2\text{CH}_3$ (26%) (eq 5), and the rest of the $\text{TMSC}\equiv\text{CTMS}$ remains unreacted. It is important to point out

that trace amounts of $\text{TMSC}\equiv\text{CSiHPh}_2$ ¹² were found using GC-MS and fully confirmed with the rest of the products by comparison with analytical samples.



When $\text{TMSC}\equiv\text{CPr}^i$ was reacted with PhSiH_3 (eq 6) ($\text{TMSC}\equiv\text{CPr}^i$: PhSiH_3 1:2) in refluxing THF, for 30 h, 68.7% of the $\text{TMSC}\equiv\text{CPr}^i$ converts to 68% TMSH , 39% $\text{HC}\equiv\text{CPr}^i$, 3.3% ${}^i\text{PrC}\equiv\text{CSiHPh}_2$, 13% *trans* ${}^i\text{PrCH}=\text{CHSiH}_2\text{Ph}$, 9.4% $({}^i\text{PrC}\equiv\text{C})_2\text{SiHPh}$, and 2% ${}^i\text{PrCH}_2\text{CH}_2\text{SiH}_2\text{Ph}$. Regarding the silane, 86.1% of PhSiH_3 reacted producing 10% Ph_2SiH_2 , 75% of oligomers via the dehydrogenative coupling of silane, and trace amounts of Ph_3SiH and SiH_4 (*caution*).²¹ As can be seen, a myriad of different products are obtained when the reactions are carried out with internal alkynes; however it is important to point out that all the products were carefully separated, analyzed, and fully confirmed via GC, GC-MS, HPLC-MS, and comparison to pure analytical samples.

(21) Wang, J.; Eisen, M. S. (manuscript in preparation).

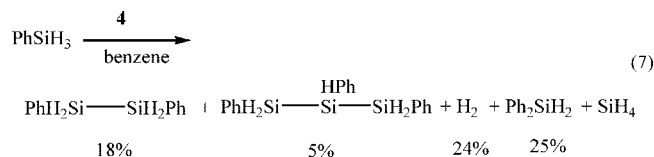
Scheme 2. Regeneration of Complexes A and B in the Formation of TMSH and the Oligomeric Silanes**Scheme 3. Proposed High-Temperature Mechanism for the Hydrogenation of Terminal Alkynes Promoted by the Hydride Complex D****Scheme 4. Plausible High-Temperature Mechanism for the Terminal C–H and the Si–C Activation Bonds in Terminal Alkynes with PhSiH₃**

A conceivable mechanism for the reactivity of the internal alkynes with PhSiH₃ promoted by complex **4** is presented in Scheme 4. The hydrogenation products and the hydrosilylation products are obtained in a similar fashion to that already observed for the organoactinide alkyl complexes starting from the corresponding hydride complex **D** (Scheme 3).^{2r,9,10,12} As

already shown above, when complex **D** reacts with the internal alkynes, at room temperature, cleaving the TMS group produces complex **A** and TMSH (Scheme 2). The acetylide complex **A** may react with the silane (depending on the regiochemistry), producing either the terminal alkyne and the corresponding complex **C** (Scheme 4) or the hydrosilylated alkyne PhSiH₂C≡CR and complex **D**. When complex **A** reacts with PhSiH₂C≡CR, PhSiH(C≡CR)₂ is produced.

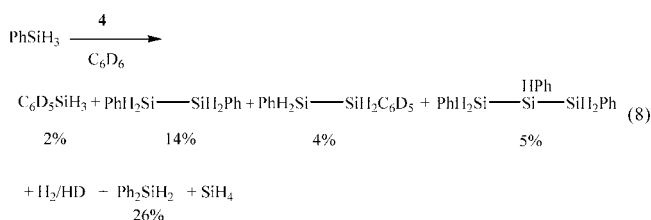
An additional activation pathway that is operative regards when complex **C** reacts with an additional molecule of PhSiH₃, in which the *Ph* moiety is cleaved, forming Ph₂SiH₂ and likely complex **F**, which upon reaction with PhSiH₃ regenerates complex **C** and forms SiH₄ (*caution: extremely flammable*) (Scheme 5). If Ph₂SiH₂ reacts with complex **F**, SiH₄ is again formed along with complex **G**, which is like complex **C** with a SiHPh₂ moiety attached to the metal. The reaction of complex **G** with PhSiH₃ will produce Ph₃SiH, cleaving again the phenyl moiety, and regenerates complex **F** as observed for TMSC≡CPr^t.

At this stage it is quite clear that the metal-oxide *n*-butyl complex can react with the silanes, activating either the phenyl or the hydrogen moieties as well as activating the terminal moiety or the triple bond of the alkynes. Hence, this unique catalytic activity of complex **4** toward the metathesis of internal silylalkynes and their silicon-containing products prompted us to explore the catalytic properties of complex **4** toward phenylsilane alone. When complex **4** was reacted with an excess of PhSiH₃ in refluxing benzene for 30 h, besides the formation of the 2 equiv of PhSiH₂Bu, it produces

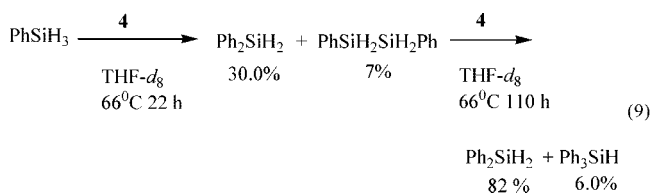


a dimer, a trimer, dihydrogen, Ph_2SiH_2 , and small amounts of SiH_4 (*caution*) (eq 7).

The unexpected formation of Ph_2SiH_2 in this reaction indicates that either one of the phenyl rings is transferred/cleaved from the starting material or the solvent is activated by the complex. To elucidate which is the main operative pathway, we decided to run the reaction in perdeuterated benzene (eq 8). The lack of formation of the deuterated SiH_3D , $\text{C}_6\text{D}_5\text{H}$, or $\text{C}_6\text{D}_5\text{SiH}_2\text{Ph}$ indicates that the perdeuterated benzene is mainly activated by an organouranium silicon complex, as presented in Scheme 6. The lack of formation of deuterated silane compounds (such as PhSiH_2D , PhSiHD_2 , or PhSiD_3) indicates that the scrambling of M–H and M–D is not operative under our reaction conditions.



When the same reaction was carried out in $\text{THF}-d_8$, disproportionation reactions of the PhSiH_3 were obtained and the amounts of the products changed as a function of time. Hence, at up to 22 h two products are mainly formed, and when the reaction was allowed to stand for 110 h, the tertiary silane Ph_3SiH was produced (eq 9).



A disproportionation mechanism for the reactivity of complex **4** with an excess of PhSiH_3 is presented in Scheme 6. The mechanism shown is a combination of simple metathesis and protonolytic reactions.¹⁵ The reaction of the hydride complex **D** with PhSiH_3 will produce in the absence of alkynes the silicon complex **C** and dihydrogen. Complex **C** can react with one more equivalent of PhSiH_3 in two competitive pathways, the first producing the dehydrogenative coupling dimer and regenerating complex **D** or inducing the unexpected phenyl metathesis, producing Ph_2SiH_2 and complex **F**, containing the U–SiH₃ moiety. Complex **F** can also react with an additional silane molecule, producing the observed SiH_4 with the regeneration of complex **C**, although if reacted with the solvent (C_6D_6), it will produce the deuteride complex **H** and $\text{C}_6\text{D}_5\text{SiH}_3$. Complex **H** reenters the catalytic cycle, forming complex **C** and HD. The formation of the trimer will be obtained if the dimer compound undergoes a metathesis with complex **C**.

In conclusion we have presented here the synthesis of two *ansa*-type organoactinide oxide-bridged complexes. In addition we have characterized an oxygen-bridged dibutyl organouranium complex and studied its unique reactivity toward silanes and terminal and internal alkynes. When comparing the different expected effects for an increased reactivity, from this research

it is quite clear that coordinative unsaturation is the main parameter for the activation of the complexes as compared to the electronic effect that is produced by the nucleophilic effect of the donating oxygen-bridged atom. It is important to point out that with the monomeric actinides of the *ansa*-type metallocenes no reactivity as shown for complex **4** was observed. Hence, the research presented here shows the first steps for the synthesis of extremely active complexes. The design and tailoring of the selectivities keeping the high activities in the activation of other coordinative unsaturated organoactinides is under investigation as well as the reactivity of the alkyl complex **4** for the hydrosilylation of alkenes.

Experimental Section

Materials and Methods. All manipulations of air-sensitive materials were performed in a high-vacuum line or in a nitrogen-filled Vacuum Atmospheres glovebox with a high-capacity recirculator. Ether solvents (DME, THF) were distilled under argon from sodium benzophenone ketyl. Hydrocarbon solvents (toluene, hexane) were distilled under argon from Na/K alloy. All solvents for vacuum line manipulations were stored in vacuo over Na/K alloy in resealable bulbs. Deuterated solvents were freeze–pump–thaw degassed and dried over Na/K alloy for 1 h. UCl_4 ²² and ligand $\text{Me}_2\text{SiCp}'_2\text{Li}_2 \cdot 2\text{DME}$ ²³ were prepared according to the literature. $\text{Me}_2\text{SiCp}'_2\text{UCl}_2 \cdot 2\text{DME} \cdot 2\text{LiCl}$ (**1**) was prepared according to a literature procedure.¹⁵

$\text{TMSC}\equiv\text{CH}$, $\text{TMSC}\equiv\text{CTMS}$, Ph_2SiH_2 , Ph_3SiH (Aldrich) and TMSH , $\text{TMSCH}_2\text{CH}_3$, SiH_4 (ABCR) were obtained commercially. The gases were used as received, and the liquids or low melting point solids were freeze–pump–thaw degassed, distilled or vacuum transferred under argon or reduced pressure, and dried by activated molecular sieves (4 Å) for 2 h. $\text{TMSC}\equiv\text{CC}_3\text{H}_7$,²⁴ $\text{Ph}_2\text{SiHC}\equiv\text{CC}_3\text{H}_7$,¹² and (*E* and *Z*)- $\text{PhSiH}_2\text{C}\equiv\text{CC}_3\text{H}_7$,^{4,12} were prepared according to the literature.

Physical and Analytical Measurements. NMR spectra were recorded on Bruker 400 and 200 MHz instruments. Chemical shifts for ¹H and ¹³C are referenced to internal solvent. NMR experiments on air-sensitive samples were conducted in J. Young Teflon valve-seal tubes. GS-MS analysis was performed on a Finnigan MAT TSQ 70 mass spectrometer. FTIR spectra were registered using a Bruker Vector 22 instrument using KBr plates. Molecular weight determinations were performed using cryoscopic Knauer Cryo equipment, in benzene. Gas measurements were performed on a Toepler pump. Elemental analyses were performed at the microanalysis laboratory of the Hebrew University of Jerusalem.

Low-temperature X-ray diffraction experiments were carried out on a Nonius-Kappa CCD diffractometer with graphite-monochromated Mo K α radiation. The crystals were placed in dry and degassed Parathon-N (Du-Pont) oil in a glovebox. Single crystals were mounted on the diffractometer under a stream of cold N₂ at 230 K. Cell refinements and data collection and reduction were carried out with the Nonius software package.²⁵ The structure solution was carried out by the SHELXS-97²⁶ and SHELXSL-97²⁷ software packages, respectively. The ORTEP program incorporated

(22) Hermann, J. A.; Suttle, J. F. *Inorg. Synth.* **1957**, 5, 143.

(23) Fendrick, C. M.; Schertz, L. D.; Day, V. W.; Marks, T. J. *Organometallics* **1988**, 7, 1828.

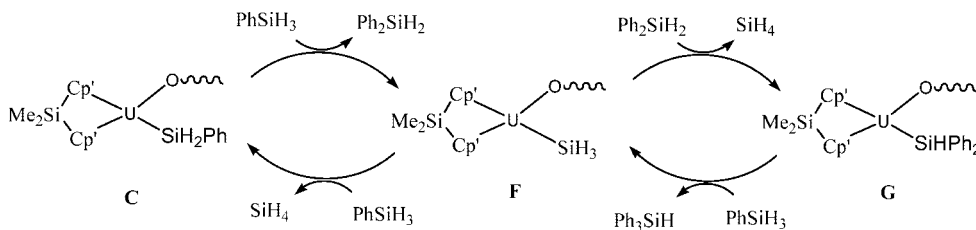
(24) Haddaway, K.; Somekawa, K.; Fleming, P.; Tossell, J. A.; Mariano, P. S. *J. Org. Chem.* **1987**, 52, 4239.

(25) Nonius 2001, Kappa CCD Collect Program for data collection, and HKL, Scalepack, and Denzo (Otwinowski & Minor, 2001) software packages for data reduction and cell refinement.

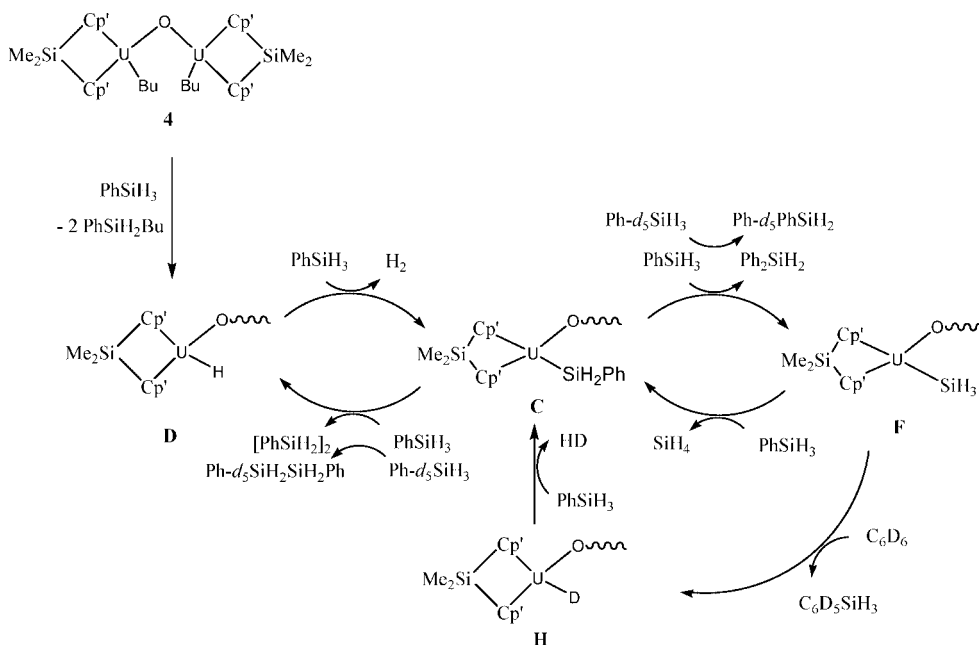
(26) Sheldrick, G. M. *Acta Crystallogr.* **1990**, A46, 467.

(27) Sheldrick, G. M. *SHELXL-97, Program for the refinement of crystal structures*; University of Göttingen: Germany, 1997.

Scheme 5. Plausible Mechanism for the Formation of SiH₄, Ph₂SiH₂, and Ph₃SiH Compounds in the Activation of Internal Alkynes Promoted by Complex 4



Scheme 6. Mechanistic Scenario for the Formation of the Metathesis Products in the Reaction of PhSiH₃ with Complex 4 in Benzene or C₆D₆^a



^a Only half the complex is depicted for clarity.

in the TEXRAY structure analysis package was used for molecular graphics.²⁸ Toepler pump data were obtained as described in the literature.²⁹

Synthesis of Complex $\{[\eta^5\text{-}(\text{C}_5\text{Me}_4)_2\text{SiMe}_2\text{UCl}]_2(\mu\text{-O})(\mu\text{-Cl})\cdot\text{Li}\cdot(\text{DME})_3\cdot\text{DME}$ (2). A 100 mL round-bottom flask equipped with a magnetic stir bar and Schlenk frit was charged in the glovebox with 0.9 g (1.03 mmol) of the orange powder of complex **1**. The frit was connected to a high-vacuum line, and DME (30 mL) containing 18.56 mg (1.03 mmol) of H₂O was condensed onto it at -78°C . The exact amount of water was measured by dissolving a much larger amount of water in 1 L of DME and then using the exact needed DME-containing water solution. Then the solution was allowed to warm to room temperature, and the volume of the solvent was next reduced until precipitation had commenced. The brown precipitate was then dissolved with heating, slowly (for 4 h) cooled to -45°C , and left at this temperature for 48 h to obtain 1.21 g (yield = 75%) of brown crystals of complex **2**. ¹H NMR (200 MHz, C₆D₆): δ -83.36 (s, 3H, CH₃), -56.05 (s, 3H, CH₃), -29.23 (s, 3H, CH₃), -26.30 (s, 3H, CH₃), 1.44 (s, 3H, CH₃), 2.84 (s, 3H, CH₃), 3.18 (s, 24H, DME), 3.60 (s, 16H, DME), 16.90 (s, 3H, CH₃), 29.50 (s, 3H, CH₃), 29.70 (s, 3H, CH₃), 43.75 (s, 3H, CH₃). ¹³C NMR (200 MHz, C₆D₆, DEPT): δ 71.4 (CH₂, DME), 54.7 (CH₃, DME), 25.71 (CH₃), -11.78 (CH₃), -37.34 (CH₃), -70.11 (CH₃), -78.32 (CH₃). IR (cm⁻¹ KBr): $1451(\text{m})$, $1380(\text{m})$,

$1328(\text{m})$, $1252(\text{s})$, $1126(\text{m})$, $1080(\text{m})$, $1018(\text{m})$, $842(\text{s})$, $816(\text{s})$, $768(\text{s})$, $675(\text{s})$, $532(\text{s})$, $455(\text{s})$, $435(\text{s})$. Anal. Calcd for complex **2**, C₅₆H₁₀₀Cl₃LiO₉Si₂U₂: C, 43.03; H, 6.45; Cl, 6.81. Found: C, 42.96; H, 6.81; Cl, 6.34. Mp (dec) = $148\text{--}153^\circ\text{C}$. Cryoscopic studies were measured on crystals washed with benzene to remove all the cocrystallized DME. *M_w* (calc for C₅₂H₉₀Cl₃LiO₇Si₂U₂ = 1472.80) found = 1348.

Synthesis of Complex $\{[\eta^5\text{-}(\text{C}_5\text{Me}_4)_2\text{SiMe}_2\text{UCl}]_2(\mu\text{-O})(\mu\text{-Cl})\cdot\text{Li}\cdot 1/2\text{DME}\}_2$ (3). A 100 mL round-bottom flask equipped with a magnetic stir bar and Schlenk frit was charged in the glovebox with 1.8 g (2.06 mmol) of the orange powder of complex **1**. The frit was connected to a high-vacuum line, and 45 mL of toluene containing 18.56 mg (1.03 mmol) of water was vacuum transferred condensed onto it at -78°C . The solution turned red-brown when allowed to warm to room temperature. The volume of the solvent was next reduced by vacuum distillation until precipitation had commenced. The precipitate was then dissolved by slow heating (for 4 h) and when a clear solution was obtained cooled to -45°C and left at this temperature for 72 h to obtain 0.87 g (yield 68%) of brown crystals of complex **3**. Mp (dec) = 117°C . IR (cm⁻¹ KBr): $1461(\text{m})$, $1452(\text{m})$, $1345(\text{m})$, $1344(\text{m})$, $1312(\text{m})$, $1300(\text{m})$, $1246(\text{s})$, $1238(\text{s})$, $1215(\text{m})$, $1114(\text{m})$, $1097(\text{m})$, $1067(\text{m})$, $1043(\text{m})$, $1032(\text{m})$, $1003(\text{m})$, $989(\text{s})$, $845(\text{s})$, $821(\text{s})$, $810(\text{s})$, $798(\text{s})$, $757(\text{s})$, $739(\text{s})$, $656(\text{s})$, $642(\text{m})$, $523(\text{s})$, $518(\text{s})$, $464(\text{sb})$, $435(\text{b})$. Anal. Calcd for complex **3**, C₈₄H₁₃₀Cl₆Li₂O₄Si₄U₄: C, 40.44; H, 5.25; Cl, 8.53; Li, 0.56. Found: C, 40.79; H, 5.71; Cl, 8.21; Li,

(28) ORTEP, TEXRAY Structure Analysis Package; Molecular Structure Corporation: The Woodlands, TX, 1999.

(29) Tzfielens, G. J.; Malfait, J. *J. Sci. Instrum.* **1965**, *42*, 28.

0.48. Mp (dec) = 127–135 °C. Cryoscopic measurements on benzene, M_w (calc) = 2494.98, found = 2195.

Synthesis of Complex (Me₂SiCp'UBu)₂O·2THF (4). Under an argon flush, 3 mL (7.32 mmol) of a solution of 2.44 M ⁿBuLi in hexane was syringed into a 100 mL two-necked round-bottom reaction flask, which was equipped with a magnetic stirring bar. The hexane was removed in vacuo until dryness at room temperature. The flask was introduced into a glovebox, connected to a swivel solid addition tube, which was charged with 2 g (0.801 mmol) of complex **3**, {[η⁵-(C₅Me₄)₂SiMe₂]UCl₂(μ-O)(μ-Cl)·Li·1/2DME}₂, and the flask was reconnected to a high-vacuum line. A 25 mL amount of DME was condensed into the ⁿBuLi at -78 °C. The solution was warmed to -30 °C, and then complex **3** was added slowly by rotating the swivel tube. The mixture was stirred at -30 °C for 2 h and then allowed to warm to 0 °C and stirred for an additional hour. The DME was then removed by vacuum at 0 °C (13 h) to yield a black solid. The solid was washed twice with 15 mL of hexane and recrystallized from cold THF to yield 0.820 g (76%). All attempts to get crystals suitable for X-ray analysis failed. Mp (dec) = 92 °C. ¹H NMR exhibited concentration and solvent dependence phenomena. ¹H NMR (200 MHz, C₆D₆): δ -6.5 (bs, $\nu_{1/2}$ = 220 Hz, 2H, CH₂-U), -1.7 (bs, 4H, U-CH₂CH₂), -0.2 (s, 6H, Me₂Si), 0.2–2.5 (bs, 10H, CH₂CH₃), 1.48 (m, 8H, THF), 1.86 (s, 12H, CH₃-Cp) 1.96 (s, 12H, CH₃-Cp), 3.6 (m, 8H, THF), 12.83 (bs, $\nu_{1/2}$ = 220 Hz, 2H, CH₂-U). ¹H NMR (200 MHz, THF-*d*₈): δ -31.75 (bs, $\nu_{1/2}$ = 50 Hz, 2H, CH₂-U), -7.85 (bs, 4H, UCH₂CH₂), 0.27 (s, 6H, Me₂Si), 1.38 (m, 8H, THF), 1.93 (s, 12H, CH₃-Cp), 1.94 (s, 12H, CH₃-Cp), 3.52 (m, 8H, THF), 10.14 (bs, 3H, CH₃), 12.85 (bs, 3H, CH₃), 20.79 (bs, 2H, CH₂), 23.75 (bs, 2H, CH₂), 38.12 (bs, 2H, U-CH₂). ¹³C NMR (50 MHz, THF-*d*₈): δ 6.5, 11.5, 14.5, 29.4 (THF), 74.8 (THF), 106.1, 110.2, 116.2. IR (KBr, cm⁻¹): 1637.3(m), 1551.7(w), 1446(s), 1384.1(s), 1305.9(5), 1249.0(s), 1224.4(m), 1188.6(w), 1113.6(w), 1077.8(w), 1045.2(m), 1025.7(w), 986.6(m), 945.0(m), 918.1(w), 898.6(w), 836(w), 810.6(w), 768.2(m), 732.4(w), 605.3(w), 432.6(m). Anal. Calcd for (Me₂SiCp'UBu)₂O·2THF, C₅₆H₉₄O₃Si₂U₂ (1347.573): C, 49.91; H, 7.03. Found: C, 50.19; H, 6.87. Mp (dec) = 135–145 °C. Cryoscopic measurements were measured in benzene after washing the complex to remove possibly labile coordinated THF. M_w (calc for C₄₈H₇₈OSi₂U₂) = 1203.36, found = 1156.

The complex is slightly soluble in methylcyclohexane, benzene, and toluene and dissolves readily in THF or other etheric solvents but is insoluble in hexane. The ¹H NMR spectrum of this paramagnetic f² uranium complex in THF-*d*₈ is complex, exhibiting large paramagnetic contact signals for the ancillary ligation Me₂Si(C₅Me₄)₂ and coordinated THF solvent molecules. The signals of the two butyl groups are broad and nonequivalent due to the plausible asymmetry formed by the coordinated THF. In benzene the signals are very well behaved, and it is possible to correlate the signals to the complex. To corroborate the existence of these alkyl moieties, complex **4** was reacted with excess amounts of PhSiH₃ to produce *only* 2 equiv of the corresponding PhSiH₂Bu. This result corroborates the presence of the two butyl groups as described in complex **4**.

General Procedure for the Catalytic Reactions. In a typical experiment, a 50 mL Schlenk tube (for low boiling point liquids or gases a heavy duty double-wall Schlenk was used) equipped with a Teflon valve was charged in the glovebox with the amount of needed catalyst **4** (10 mg, 7.42 μmol). On the vacuum line, 5 mL of solvent and the required amount of alkyne or alkynes (and/or silane) were vacuum transferred into the Schlenk tube (high boiling point liquids and solids were inserted into the glovebox). The progress of the reaction was monitored by GC-MS and GC chromatography and corroborated by ¹H NMR spectroscopy. Gases and low boiling point liquids produced in the reaction were vacuum transferred at low temperatures to new J-Young NMR tubes and

sealed to measure the ratio of the compounds. The total amount of gases was measured with a Toepler pump. All the compounds were separated via preparative GC chromatography using a preparative 1/4 in. × 4 m OV 101 column or 1/4 in. × 4 m Carbowax 20 M equipped with a TCD detector. The separated compounds were measured with GC-MS and NMR comparing to pure analytical samples. The new reaction products' structures were characterized by ¹H NMR and ¹³C{H} NMR spectrometry and by GC and GC-MS chromatography. **Caution: SiH₄ is a flammable gas that reacts in open air!** Products for comparison were either prepared in the laboratory following known procedures or commercially purchased.

Reaction of TMSC≡CH with PhSiH₃ Promoted by Complex 4. According to the general process 0.79 mL (7.78 mmol) of TMSC≡CH reacted with 0.96 mL (7.78 mmol) of PhSiH₃ in a 5 mL solution of THF at room temperature for 200 h to yield 20.9 mL (12%) of TMSH, 502.5 mg (38%) of TMSC≡CTMS, and 87.2 mL (50%) of HC≡CH in addition to 426 mg (76% based on PhSiH₃) of oligomeric polysilane. When the same reaction was carried out at 60 °C for 60 h, 232.1 mg (30%) of TMSCH=CH₂, 182 mg (23%) of TMSCH₂CH₃, 304.3 mg (23%) of TMSC≡CTMS, and 40.1 mL (23%) of HC≡CH in addition to 403 mg of oligomeric silanes were produced.

Reaction of TMSC≡CTMS with PhSiH₃ Promoted by Complex 4. According to the general process, 275 mg (1.62 mmol) of TMSC≡CTMS reacted with 0.40 mL (3.21 mmol) of PhSiH₃ in 5 mL of THF at 66 °C for 47 h to yield 9.43 mL (26%) of TMSH and 42.9 mg (26%) of TMSCH₂CH₃. 84% of PhSiH₃ gives 219 mg (63%) of oligomers, 65.6 mg (11%) of Ph₂SiH₂, and 7.25 mL (10%) of SiH₄.

Reaction of TMSC≡CPrⁱ with PhSiH₃ Promoted by Complex 4. On the basis of the general process, the reaction of 210 mg (1.5 mmol) of TMSC≡CPrⁱ with 0.37 mL (3.0 mmol) of PhSiH₃ was carried out at 66 °C for 30 h. 68.7% of the TMSC≡CPrⁱ reacts giving 39.8 mg (39%) of ⁱPrC≡CH, 12.5 mg (3.3%) of ⁱPrC≡CSiHPh₂ 34.3 mg (13.%) of *trans* ⁱPrCH=CHSiH₂Ph, 33.8 mg (9.4%) of (ⁱPrC≡C)₂SiHPh, 5.3 mg (2%) of ⁱPrCH₂CH₂SiH₂Ph, and 22.11 mL (67%) of TMSH. 86.1% of the rest of PhSiH₃ gave 10% Ph₂SiH₂, trace amounts SiH₄ and Ph₃SiH, and 243 mg (75%) of oligomeric (PhSiH)_{*x*}.

Spectroscopic data for (ⁱPrC≡C)₂SiHPh: ¹H NMR (200 MHz, C₆D₆): δ 7.74–7.81 (m, 2H, *m*-H-Ph), 7.21–7.30 (m, 3H, *o*-*p*-H-Ph), 5.15 (s, 1H, SiHPh), 2.22 (septet, *J* = 6.95 Hz, 2H, CHPrⁱ), 1.10 (d, *J* = 6.95 Hz, 12H, CH(CH₃)₂). ¹³C NMR (50 MHz, C₆D₆): δ 135.2, 129.9, 128.3 (s, CH-Ph), 132.4 (s, CC₃H₅), 98.1 (s, C≡C), 68.5 (s, C≡C), 34.6 (s, CHMe₂), 22.8 (s, CH(CH₃)₂). ²⁹Si NMR (79.5 MHz, C₆D₆): δ 9.3 (s, PhSiH). GC-MS: *m/z* 240 (M⁺), 239 (M⁺ - H), 184 (M⁺ - ⁱPr - CH), 105 (PhSi⁺, 100%). HRMS calcd for C₁₆H₂₀Si = 240.4155, found = 240.4139. Anal. Calcd: C, 79.93; H, 8.38. Found: C, 79.59; H, 8.11.

Spectroscopic data for ⁱPrCH₂CH₂SiH₂Ph: ¹H NMR (200 MHz, C₆D₆): δ 7.69–7.81 (m, 2H, *m*-H-Ph), 7.19–7.33 (m, 3H, *o*-*p*-H-Ph), 5.15 (t, *J* = 2.77 Hz, 2H, SiH₂Ph), 2.18 (m, 1H, CH(CH₃)₂), 1.34 (m, 2H, CHCH₂CH₂), 1.02 (d, *J* = 6.95 Hz, 6H, CH(CH₃)₂), 0.85 (tt, *J* = 6.95 Hz, *J* = 2.77 Hz, 2H, CH₂CH₂SiH₂). ¹³C NMR (50 MHz, C₆D₆): δ 135.2, 129.9, 128.3 (s, CH-Ph), 122.4 (s, CC₃H₅), 37.4 (s, (CH₂Ph), 34.6 (CHMe₂), 22.8 (s, CH(CH₃)₂), 10.4 (s, CH₂Si). ²⁹Si NMR (79.5 MHz, C₆D₆): δ 8.5 (t, *J* = 210 Hz, SiH₂). GC-MS: *m/z* 178 (M⁺), 177 (M⁺ - H), 135 (M⁺ - CH(CH₃)₂), 107 (M⁺ - ⁱPr - CH₂CH₂), 105 (PhSi⁺, 100%). HRMS calcd for C₁₁H₁₈Si = 178.1177, found = 178.1156. Anal. Calcd for C₁₁H₁₈Si: C, 74.08; H, 10.17. Found: C, 73.75; H, 9.89.

Reaction of PhSiH₃ Promoted by Complex 4. Based on the general process, the reaction of 0.37 mL (3.0 mmol) of PhSiH₃ was carried out in refluxing benzene for 30 h, giving 115.6 mg of dimer (18%), 48 mg of trimer (5%), 138 mg of Ph₂SiH₂ (25%), and 24% H₂.

According to the typical experimental procedure, 0.09 mL of PhSiH₃ (0.73 mmol) promoted by complex **4** in refluxing C₆D₆ for 30 h gave C₆D₅SiH₃ (2.2%), PhSiH₂SiH₂Ph dimer (13.8%), trimer (5.1%), Ph₂SiH₂ (25.8%), C₆D₅SiH₂SiH₂Ph (3.6%), and SiH₄ and H₂/HD.

C₆D₅SiH₃: GC-MS (70 eV, EI, relative intensity) *m/e* 113(18), 99(10), 86(40), 85(58), 84(50), 83(100), 82(50), 81(54), 79(28).

C₆D₅SiH₂SiH₂Ph: ²H NMR (C₇H₈, 400 MHz) δ 7.28, 7.15. GC-MS (70 eV, EI, relative intensity): *m/e* 218(11), 213(15), 189(22), 183(93), 105(100).

According to the typical experimental procedure, 0.09 mL of PhSiH₃ (0.73 mmol) promoted by complex **4** in refluxing THF-*d*₆ for 22 h gave dimer (7%) and Ph₂SiH₂ (30%), for 44 h to give

dimer (8%) and Ph₂SiH₂ (42%), for 66 h to give Ph₂SiH₂ (56%), and for 110 h to give Ph₂SiH₂ (82%) and Ph₃SiH (6%).

Acknowledgment. This research was supported by the Israel Science Foundation Administrated by the Israel Academy of Science and Humanities under contract 1069/05.

Supporting Information Available: X-ray diffraction data cif files for complexes **2** and **3**. This material is available free of charge via the Internet at <http://pubs.acs.org>.

OM800418U